



Published in final edited form as:

*J Med Primatol.* 2016 February ; 45(1): 21–27. doi:10.1111/jmp.12204.

## Artifact correction in diffusion MRI of non-human primate brains on a clinical 3T scanner

Xiaodong Zhang<sup>1,2</sup>, John E. Kirsch<sup>3</sup>, Xiaodong Zhong<sup>4</sup>

<sup>1</sup>Yerkes Imaging Center, Yerkes National Primate Research Center, Emory University, Atlanta, Georgia 30329

<sup>2</sup>Division of Neuropharmacology and Neurologic Diseases, Yerkes National Primate Research Center, Emory University, Atlanta, Georgia 30329

<sup>3</sup>MR Division, Siemens Healthcare, Cary, NC, USA

<sup>4</sup>MR R&D Collaborations, Siemens Healthcare, Atlanta, GA, USA

### Abstract

**Introduction:** Smearing artifacts were observed and investigated in diffusion tensor imaging (DTI) studies of macaque monkeys on a clinical whole body 3T.

**Methods:** Four adult macaques were utilized to evaluate DTI artifacts. DTI images were acquired with a single-shot echo-planar imaging (EPI) sequence using parallel imaging.

**Results:** The smearing artifact observed on the diffusion-weighted images and fractional anisotropy maps was caused by the incomplete fat suppression due to the irregular macaque frontal skull geometry and anatomy. The artifact can be reduced substantially using a novel three-dimensional (3D) shimming procedure.

**Conclusion:** The smearing artifacts are caused by the incomplete fat suppression due to the irregular structure of macaque frontal skull. The artifact can be reduced significantly using a robust 3D shimming approach. The DTI protocol combined with the shimming procedure could be a robust approach to examine brain connectivity and white matter integrity of non-human primates using a conventional clinical scanner.

### Keywords

DTI; GRAPPA; susceptibility artifact; non-human primate; chemical shift artifact; fat suppression; parallel imaging

---

Correspondent to: Xiaodong Zhang, PhD, Yerkes Imaging Center, Yerkes National Primate Research Center, Emory University, 954 Gatewood Rd NE, Atlanta GA 30329, Xzhang8@emory.edu, Tel: 404-712-9874, Fax: 404-712-9917.

Ethical standards: The manuscript does not contain clinical studies or patient data.

Disclosure: The authors declare that they have no conflict of interest.

## Introduction:

As non-human primate (NHP) brains are structurally and functionally similar to the human brain, NHPs are popularly used in a wide range of neuroscience and disease studies including Human Immunodeficiency Virus (HIV), stroke, Huntington's disease (HD), Alzheimer's disease (AD), aging, drug addiction, and autism. Diffusion tensor imaging (DTI) is able to assess the white matter integration and brain connectivity, and has been increasingly used in various NHP studies [1–7], demonstrating its novel capacity and robustness in NHP researches.

DTI data acquisition is usually conducted with the spin-echo echo-planar imaging (EPI) sequence in either clinical or preclinical studies. Due to the inherent property of the EPI sequence, DWI images are very vulnerable to motion or susceptibility issues, resulting in various artifacts such as ghost, signal drop-off, and distortion [8–11]. The motion artifacts can be well controlled in anesthetized animals. However, other artifacts may become worse in high (3T or above) or ultrahigh (7T or above) field scanners due to reduced T2 and increased susceptibility effects compared to 1.5T scanners. Since there are few research MRI scanners dedicated for NHP studies, NHP (such as macaque monkeys) studies are usually conducted on high-field whole body clinical scanners. NHP brains are much smaller than human's (1200–1300cc in human, ~400cc in chimpanzee, and ~100cc in macaque monkey) and require smaller field of view (FOV) and increased spatial resolution. In particular, the DTI images can be compromised with severe T2\* effect due to the increased echo time as stronger gradients are demanded in diffusion MRI scans. Because clinical scanners usually are equipped with low strength gradient (4G/m) compared with a standard research scanner (40G/m), the detrimental T2\* effect in NHP brain imaging can be more deteriorated with a high (or ultrahigh) field clinic setting.

Previous studies have demonstrated that parallel imaging is an effective and robust approach to improve the DTI image quality of human or NHP brains in clinical scanners [12–15]. However, a new type of image artifact, referred as the “smearing artifact” in this work, was sometimes observed in our DTI study of NHP brains. To our best knowledge, such smearing artifact has not been reported in previous human or animal DTI studies. In the present study, the smearing artifact was investigated and a solution was proposed.

## Materials and Methods:

Adult rhesus monkeys (n = 4, all female, 9–10 years old, 7–11 kg) were utilized. Each subject was initially anesthetized with 3–5mg/kg of telazol or 10mg/kg of ketamine, and then placed on a temperature-controlled heating pad, and intubated and breathed on its own under ~1% isoflurane delivered to a non-rebreathing circuit. The head of the subject was immobilized with a home-built head holder and placed in the supine position during MRI scanning. All major physiological parameters were monitored and maintained in normal ranges [16]. All procedures were approved by the Institutional Animal Use and Care Committee at Emory University in a facility accredited by AAALAC and in compliance with the Animal Welfare Act and the Public Health Service Policy on Humane Care and Use of Laboratory Animals.

DTI images were acquired on a Siemens 3T clinical scanner (MAGNETOM Trio, a TIM system, Siemens Healthcare, Erlangen, Germany) with an 8-channel high-resolution phased-array knee coil (Invivo Inc., FL). A single-shot EPI sequence was performed, and the imaging parameters included GRAPPA on (acceleration factor = 3) or off, TR = 5000ms, TE = 80ms, field of view (FOV) = 96mm × 96mm, image matrix = 64 × 64, slice thickness = 1.5mm, 30 directions with b-value = 1000s/cm<sup>2</sup>. T1-weighted images were collected with 3D magnetization-prepared gradient-echo (MP-RAGE) sequence with the parameters: TR = 2500ms, TE = 3.33ms, FOV = 96mm × 96mm, flip angle = 8 degree, TI = 950ms, image matrix = 192 × 192, slice thickness = 1mm, 112 slices.

During the data acquisition, the B<sub>0</sub> field was first shimmed with the commercially available, vendor-offered default shimming mechanism, which was automatically initiated when starting the “localizer” scan. With the default shimming process, B<sub>0</sub> field maps were initially obtained at a defined reference starting set of 1<sup>st</sup> and 2<sup>nd</sup> order shim settings using a low spatial resolution three-dimensional (3D) double-echo steady state (DESS) acquisition [17, 18] with both echoes defined so that fat and water magnetizations were in phase. The scanning parameters of the 3D DESS acquisition included 500mm × 375mm × 500mm volume and image matrix = 64 × 48 × 64, resulting in a voxel size of 7.8 × 7.8 × 7.8 mm<sup>3</sup>. Phase difference maps computed from the two echoes produced the initial B<sub>0</sub> field map. A localized adjustment volume subset defined by the slices to be acquired was then used to calculate the optimal shim settings within this volume.

Whenever the smearing artifacts were observed in DTI scans, a specific alternative shim sequence called GRESHIM was immediately used and the diffusion scan was repeated. In this GRESHIM sequence, a field map was generated from a single-slab dual-echo 3D gradient echo (GRE) acquisition with two in-phase echo times with respect to fat and water, and then used to calculate the shim currents to improve B<sub>0</sub> homogeneity [19]. The scanning parameters of the GRESHIM sequence included FOV = 120 mm × 120 mm × 64 mm, image matrix = 256 × 256 × 64, TR=13 ms, TE = 4.1ms, flip angle = 35 degree. The field map estimation and B<sub>0</sub> inhomogeneity correction were conducted inline on the scanner.

All DTI data processing was performed using the Syngo software on the Siemens scanner console.

## Results:

The smearing artifacts were noticed within the brain regions in the fractional anisotropy (FA) maps and DWI images of adult macaque monkeys. Representative FA maps with the smearing artifacts are illustrated in Fig 1. The smearing artifacts occurred specifically in the phase-encoding direction.

Further observation in the DTI data of adult macaques revealed such artifacts were not seen in the same brain regions of DWI images without GRAPPA (Fig 2A–B), but were evident when the parallel imaging technique (GRAPPA) was applied (Fig 2C–D) and varied with different GRAPPA acceleration factors (data not shown).

Adult macaque heads show much more pronounced supraorbital ridges than the human head and are wrapped with thick muscles (Fig 3A–B). When the smearing artifacts appeared, the field map analysis indicated poor shimming in the frontal skull by the default shimming procedure (Fig 3C), resulting in incomplete fat suppression and additional muscle signal reduction in the frontal area of T1-weighted images with fat suppression (Fig 3D). After applying the GRESHIM procedure, the B0 field was improved substantially, particularly in the frontal area, as shown in the field map (Fig 3E) and corresponding T1-weighted images (Fig 3F).

As a result, the smearing artifacts were reduced substantially in the DWI images after performing the specific re-shimming. As seen in Fig 4, one DTI data set of an adult macaque is shown to demonstrate the diffusion-weighted images with artifacts (Fig 4A) and without artifacts (Fig 4B) and the corresponding FA maps (Fig 4C).

## Discussion:

In this study we investigated the smearing artifacts observed in DTI images of macaque brains scanned using parallel imaging technique on a high field clinical scanner. It is found that the artifacts are resulted from the residual fat signal due to incomplete fat suppression caused by the irregular geometry and anatomical structure of the frontal skull in NHPs. The artifact stains the brain FA maps and invalidates the DTI data analysis, but it can be reduced substantially with a specific B0 shimming procedure called GRESHIM.

Clinical scanners are designed specifically for human purpose and are usually configured with low strength gradient coils (4G/cm, slew rate = 200T/m/s). As an adult macaque monkey brain is much smaller than an adult human brain (~100cc vs ~1300cc), the spatial resolution must be increased substantially to obtain an acceptable image of a macaque brain, and accordingly results in increased echo time (TE) due to the requisite longer duration of the gradient pulsing. In addition, the TE will be elongated even more in DTI pulse sequences due to the demand of high gradient strength.

EPI images are usually degraded with distortion and signal drop-off in the tissues near regions with strong tissue susceptibility differences such as bone, sinus, and nasal cavities in the head. As seen in Fig 2A, the frontal part of the EPI images is seriously distorted and result in artifacts in the corresponding regions of FA maps (Fig 2B). After GRAPPA was applied, the image distortion was mitigated significantly (Fig 2C), but the smearing artifacts in the DWI images and FA maps of the brain remained (Fig 2C–D).

Previous studies have demonstrated that using parallel imaging technique can substantially reduce the susceptibility effect in DTI images of the macaque brain in a clinical setting. However, such benefits from parallel imaging technique are hindered because of the image artifacts reported in the present study for NHPs, invalidating the pixel-wise data analysis of DWI images and FA maps in the affected brain regions for brain connectivity or tractography study (Fig 2C–D).

The brain volume of an average adult macaque is much smaller than that of an adult human brain. Meanwhile, a macaque skull is much smaller than a human's and has irregular

geometry and anatomy compared to the human's. Especially, the supraorbital ridges of a macaque skull are much more pronounced than in a human skull which is larger and more rounded (Fig 3A–B). The heterogeneous structures of a macaque frontal head consist of frontal sinus, bones, fatty skins, bone marrow, muscle and exhibit a large area on the top of the frontal lobe, making the susceptibility effect much worse than that seen in the similar region of a human brain MRI image [20].

Further field map and T1-weighted imaging with and without fat suppression (Fig 3) suggested that the default field shimming (which is always automatically applied when starting scanning a new subject) works well in human brain scanning, but fail in macaque brain scanning (Fig 3C), causing evident B0 inhomogeneities and invalidated the fat suppression in the anterior head structure in T1-weighted imaging (Fig 3D). Fat suppression in this study was conducted using spectrally-selective RF pulses by default. Due to the field inhomogeneities, the fat signal from the B0-altered regions could not be suppressed effectively and resulted in residual fat signal (seen in T1-weighted images). Therefore, the DWI images and FA maps were contaminated with the residual fat signal due to chemical shift artifact, which was further complicated by the parallel imaging reconstruction algorithm.

In comparison with the conventional spectrally-selective fat saturation (a default mode in most clinical scanners), the Spectrally Adiabatic Inversion Recovery (SPAIR) technique uses a spectrally selective adiabatic inversion pulse to excite only fat spins and is insensitive to B1 inhomogeneity and available in most clinical scanners. With our experience in macaque brain imaging, the smearing artifact can be reduced slightly by using SPAIR, but not completely. This indicates that the B0 inhomogeneity is a major issue, not B1 inhomogeneity (data not shown).

The default shimming package in the Siemens clinical scanner is hardcoded with a fixed encoding spatial resolution of 7.8mm x 7.8mm x 7.8mm voxels, providing adequate shimming for imaging human subjects. It is hypothesized that this low spatial resolution fails to converge on an optimal shimming solution in macaque brain scanning due to the over 10-fold brain volume difference compared to human brain volume, and especially in regions containing localized susceptibility distortions. Also, as seen in our study, the B0 shimming status in the affected region could not be improved evidently by applying additional manual global shimming. Even though manual shimming in the affected region could improve the local B0 homogeneity in the affected region, but it alters the shimming status in other brain regions and can be very time-consuming and therefore increase the duration of anesthesia administration which can be a serious concern in NHP studies.

In contrast, the GRESHIM shimming procedure is based upon the GRE dual-echo acquisition with higher spatial resolution to estimate the B0-map and apply compensatory shim currents to reduce the local static field perturbation. The entire procedure is automatic and takes less than 1 minute. As shown in the present study, by using the novel GRESHIM shimming procedure, the entire B0 field can be improved substantially (Fig 3E), and so is the fat suppression efficacy around the frontal skull area (Fig 3F). As a result, the artifacts seen in DTI scans were reduced significantly and clean FA maps were achieved to ensure the

success of further data analysis. Also, the DTI protocol with 30 gradient directions was used as an example in the present study to illustrate the image artifacts and evaluate the effectiveness of the artifact correction. As a future plan, the shimming procedure can be included in other DTI protocols with more gradient directions for better evaluation of white matter integrality or fiber tractography.

Sometimes the smearing artifact is not well pronounced in original DWI images (Fig 4) and may be overseen in data acquisition. Due to the large amount of DTI data acquisition or subjects, a lot of DTI data processing are carried out automatically with dedicated software such as FSL([www.fmrib.ox.ac.uk/fsl](http://www.fmrib.ox.ac.uk/fsl)). As such automatic data analysis procedure is not able to detect the artifacts in the original DWI images, the derived DTI results could be biased with the smearing artifact. Therefore, we suggest checking the field map first before a DTI scan of a NHP brain.

Clinical high-field scanners have been equipped with increasing receiving channels to accelerate data acquisition or improve data quality using paralleling imaging technique. Due to their popularity and convenience in animal handling and experimental setting, they have been increasingly used for imaging various animals including various NHPs such as chimpanzee, macaque, squirrel monkey, marmoset or other smaller species like rodents. The anatomical dimension and geometry of NHP heads are generally irregular and very different from the human's and may result in such image artifacts in DTI or other susceptibility-vulnerable imaging modality scans. Due to the limited sample size in most NHP studies, one poor image data set may affect the significance in group comparison analysis. Therefore, it is critical to ensure the high quality of each DTI acquisition. Obviously, the smearing image artifacts could be solved with the proposed shimming procedure. In addition, DTI is a novel tool to evaluate the brain connectivity and white matter integrity but it is unable to delineate the crossing fibers within an individual voxel. In contrast, Q-ball imaging (QBI) [21], high angular resolution diffusion imaging (HARDI) [22], and diffusion spectrum imaging (DSI) [23, 24] can resolve fibers crossing but demand larger pulsed field gradients. Due to the gradient strength limitation on a clinical setting, such susceptibility-induced artifact can become even worse because of the increased TE for the demand of high b-values. Therefore, the proposed solution will be an effective approach to eliminate the image susceptibility-associated artifacts in these diffusion-MRI studies when using a clinical scanner to scan NHP brains. Certainly, the specific shimming procedure is not limited to the specific MRI scanner used in the present study but also can be adapted in the clinical scanners with other brands and models to facilitate MRI examination of small animal subjects.

## Conclusion

The irregular front skull geometry and anatomical structure of the macaque head results in incomplete fat suppression and detrimental smearing artifact in DTI images of macaque brains on a clinical setting. By using the robust GRESHIM shimming approach, the artifact can be eliminated substantially. In addition, such automatic shimming procedure could be promising to improve the local shimming and reduce image artifacts in other susceptibility-vulnerable MRI modalities (functional MRI, DSI, susceptibility-weighted imaging, et al) for examining various NHP disease models.

## Acknowledgements:

The authors thank Sudeep Patel for MRI data collection, Ruth Connelly and Doty Dempt (DVM) for animal care, the diagnosis analysis of the scanner hardware by the Siemens engineers including Keith Ball, Stephen Dayringer, Kevin Tieman, and Drs Mar Sanchez and Leonard Howell for their excellent assistance with this study. This project was supported in part by NCRR and currently by the Office of Research Infrastructure Programs of NIH (OD P51OD011132, P51RR000165 and OD P51OD011132).

## References

1. Li C, Zhang X, Komery A, Li Y, Novembre FJ, Herndon JG: Longitudinal diffusion tensor imaging and perfusion MRI investigation in a macaque model of neuro-AIDS: a preliminary study. *Neuroimage* 2011, 58(1):286–292. [PubMed: 21658455]
2. Liu Y, D'Arceuil HE, Westmoreland S, He J, Duggan M, Gonzalez RG, Pryor J, de Crespigny AJ: Serial diffusion tensor MRI after transient and permanent cerebral ischemia in nonhuman primates. *Stroke* 2007, 38(1):138–145. [PubMed: 17122422]
3. Howell BR, Godfrey J, Gutman DA, Michopoulos V, Zhang X, Nair G, Hu X, Wilson ME, Sanchez MM: Social Subordination Stress and Serotonin Transporter Polymorphisms: Associations With Brain White Matter Tract Integrity and Behavior in Juvenile Female Macaques. *Cerebral Cortex* 2013.
4. Liu X, Zhu T, Gu T, Zhong J: A practical approach to in vivo high-resolution diffusion tensor imaging of rhesus monkeys on a 3-T human scanner. *Magn Reson Imaging* 2009, 27(3):335–346. [PubMed: 18768280]
5. Adluru N, Zhang H, Fox AS, Shelton SE, Ennis CM, Bartosic AM, Oler JA, Tromp do PM, Zakszewski E, Gee JC et al.: A diffusion tensor brain template for rhesus macaques. *Neuroimage* 2012, 59(1):306–318. [PubMed: 21803162]
6. Rilling JK, Glasser MF, Preuss TM, Ma X, Zhao T, Hu X, Behrens TE: The evolution of the arcuate fasciculus revealed with comparative DTI. *Nat Neurosci* 2008, 11(4):426–428. [PubMed: 18344993]
7. Logothetis NK: MR imaging in the non-human primate: studies of function and of dynamic connectivity. *Curr Opin Neurobiol* 2003, 13(5):630–642. [PubMed: 14630229]
8. Horsfield MA: Mapping eddy current induced fields for the correction of diffusion-weighted echo planar images. *Magn Reson Imaging* 1999, 17(9):1335–1345. [PubMed: 10576719]
9. Chen B, Guo H, Song AW: Correction for direction-dependent distortions in diffusion tensor imaging using matched magnetic field maps. *Neuroimage* 2006, 30(1):121–129. [PubMed: 16242966]
10. Ardekani S, Sinha U: Geometric distortion correction of high-resolution 3 T diffusion tensor brain images. *Magn Reson Med* 2005, 54(5):1163–1171. [PubMed: 16187289]
11. Mohammadi S, Nagy Z, Hutton C, Josephs O, Weiskopf N: Correction of vibration artifacts in DTI using phase-encoding reversal (COVIPER). *Magn Reson Med* 2012, 68(3):882–889. [PubMed: 22213396]
12. Zhang X, Tong F, Li CX, Yan Y, Nair G, Nagaoka T, Tanaka Y, Zola S, Howell L: A fast multiparameter MRI approach for acute stroke assessment on a 3T clinical scanner: preliminary results in a non-human primate model with transient ischemic occlusion. *Quant Imaging Med Surg* 2014, 4(2):112–122. [PubMed: 24834423]
13. Nana R, Zhao T, Hu X: Single-shot multiecho parallel echo-planar imaging (EPI) for diffusion tensor imaging (DTI) with improved signal-to-noise ratio (SNR) and reduced distortion. *Magn Reson Med* 2008, 60(6):1512–1517. [PubMed: 19025894]
14. Jaermann T, Crelier G, Pruessmann KP, Golay X, Netsch T, van Muiswinkel AM, Mori S, van Zijl PC, Valavanis A, Kollias S et al.: SENSE-DTI at 3 T. *Magn Reson Med* 2004, 51(2):230–236. [PubMed: 14755645]
15. Bhagat YA, Emery DJ, Naik S, Yeo T, Beaulieu C: Comparison of generalized autocalibrating partially parallel acquisitions and modified sensitivity encoding for diffusion tensor imaging. *AJNR Am J Neuroradiol* 2007, 28(2):293–298. [PubMed: 17296998]

16. Li CX, Patel S, Auerbach EJ, Zhang X: Dose-dependent effect of isoflurane on regional cerebral blood flow in anesthetized macaque monkeys. *Neurosci Lett* 2013, 541:58–62. [PubMed: 23428509]
17. Bruder H, Fischer H, Graumann R, Deimling M: A new steady-state imaging sequence for simultaneous acquisition of two MR images with clearly different contrasts. *Magn Reson Med* 1988, 7(1):35–42. [PubMed: 3386520]
18. Heid O: Method and apparatus for shimming a magnet system of a nuclear magnetic resonance tomography system. US Patent #5614827 1997.
19. Proceedings of the Rapid fieldmap estimation for cardiac shimming: 2009.
20. Zhang X, Heberlein K, Sarkar S, Hu X: A multiscale approach for analyzing in vivo spectroscopic imaging data. *Magn Reson Med* 2000, 43(3):331–334. [PubMed: 10725873]
21. Tuch DS, Wisco JJ, Khachaturian MH, Ekstrom LB, Kotter R, Vanduffel W: Q-ball imaging of macaque white matter architecture. *Philos Trans R Soc Lond B Biol Sci* 2005, 360(1457):869–879. [PubMed: 16087432]
22. Tuch DS, Reese TG, Wiegell MR, Makris N, Belliveau JW, Wedeen VJ: High angular resolution diffusion imaging reveals intravoxel white matter fiber heterogeneity. *Magn Reson Med* 2002, 48(4):577–582. [PubMed: 12353272]
23. Wedeen VJ, Wang RP, Schmahmann JD, Benner T, Tseng WY, Dai G, Pandya DN, Hagmann P, D’Arceuil H, de Crespigny AJ: Diffusion spectrum magnetic resonance imaging (DSI) tractography of crossing fibers. *Neuroimage* 2008, 41(4):1267–1277. [PubMed: 18495497]
24. Meng Y, Zhang X: In vivo diffusion spectrum imaging of non-human primate brain: initial experience in transcallosal fiber examination. *Quantitative imaging in medicine and surgery* 2014, 4(2):129–135. [PubMed: 24834425]



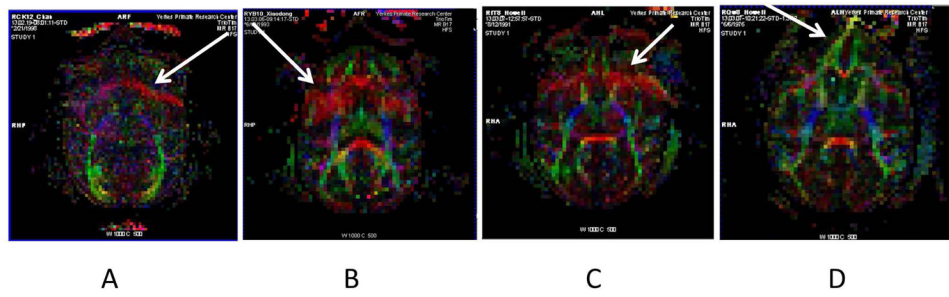


**Fig 1.** Representative FA maps contaminated with artifacts in macaque brains. A, B, C: acquired with anterior-posterior phase-encoding direction; D: acquired with left-right phase-encoding direction. Artifacts are marked with arrows.

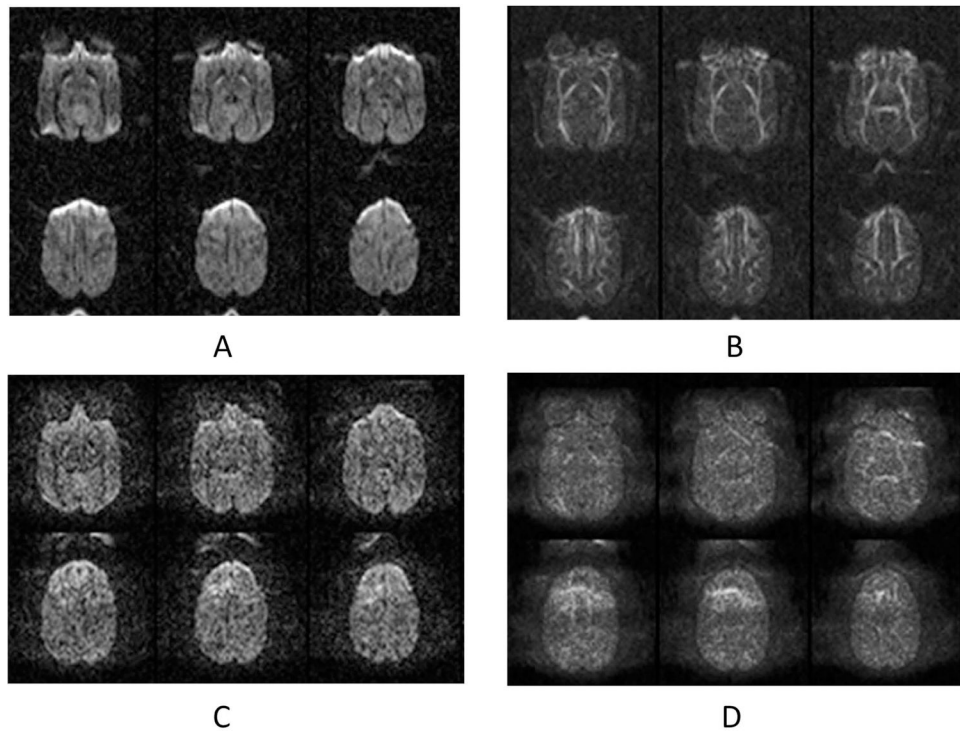


**Fig 2.** Diffusion-weighted images (DWI) of an adult macaque brain. A: DWI images acquired without GRAPPA; B: FA maps of data in A; C: DWI images acquired with GRAPPA (acceleration factor = 3); D: FA maps of data in C.

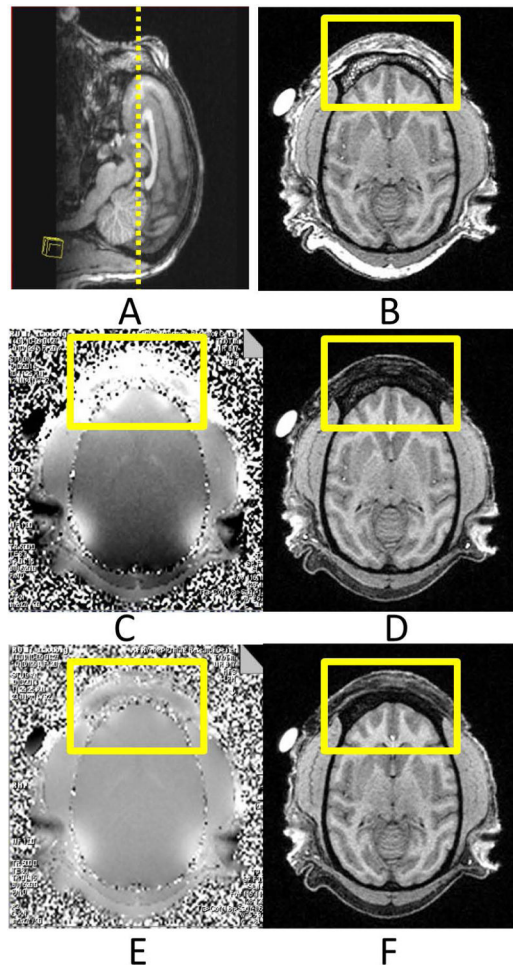


**Fig 3. Structural images of an adult macaque head. A: Sagittal T1-weighted structural Image of the monkey head. B: Axial T1-weighted image without fat suppression; C: The original field map; D: T1-weighted image with fat suppression; E: The field map after re-shimming with GRESHIM; F: T1-weighted image with fat suppression. The square boxes show the interested area with susceptibility effects.**

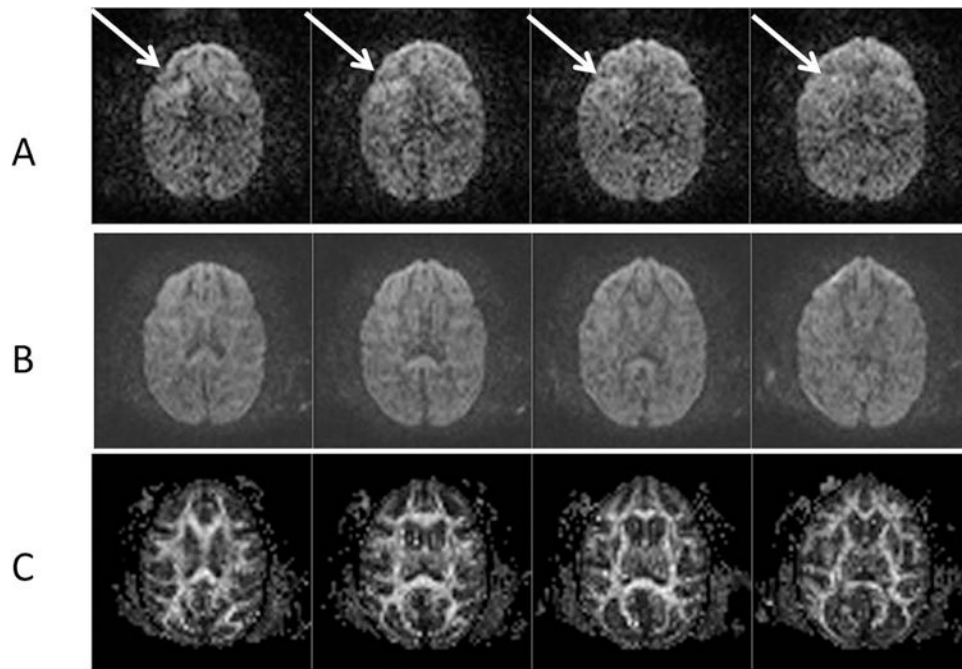


**Fig 4. Diffusion-weighted images and FA maps of an adult macaque brain.**

A: Normal axial images with FOV = 96 mm × 96mm and phase-encoding in anterior-posterior; Image artifacts are marked with arrows.

B: After B0 shimming correction with GRESHIM (4 averages); C: FA maps of DTI images after B0-shimming correction.